Modelling transport of salts through ceramic Nanofiltration membranes

Rasha Hajarat, Alec James

School of chemical engineering and analytical science, The University of Manchester

Abstract

Nanofiltration membrane can be described by Nernest-Planck equation, where separation is a result of concentration, electrical and pressure gradients across the membrane. Ceramic Nanofiltration was used to study the effect of a cation and an anion on the separation behaviour. It was noticed from the theoretical solution that the rejection of Cl^{1-} was higher than the rejection of Na^{1+}. The rejection of Na^{1+} and Cl^{1-} ions increased as the volumetric flux based on membrane area (*Jv*) increased. Also the concentration of Na^{1+} and Cl^{1-} ions inside the membrane active layer decreased as the volumetric flux based on membrane area (*Jv*) increased. In addition, the rejection of Na^{1+} and Cl^{1-} ions decreased as the feed concentration increased.

Keyword: *nanofiltration, membrane, ions, modelling.*

Corresponding author fax : 009623237238 / ext: 3097
Tel : 00962795277011
Email : r.hajarat@engineer.com

1 Introduction

The need for clean water is increasing and because of the limited water resources which require relatively little treatment to be made potable, it is becoming necessary to consider alternate sources that cannot be accessed by conventional water treatment techniques. One of the newer processes that can be used in clean water production processes is Nanofiltration which uses membranes with properties lying between those of ultrafiltration and reverse osmosis membranes. Nanofiltration membranes have the potential to be used in many different applications such as water softening, removal of hardness, removal of natural organic matter, removal of heavy metals, removal of viruses and bacteria, and the concentration of organic dyes. The permeation of ions through nanofiltration membrane can be described by using the extended Nernst-Planck equation, where it describes the solute concentration change inside the membrane and the change between the feed and the permeate concentrations. The extended Nernst-Planck equation describes the transport of ions through nanofiltration membrane in terms of concentration gradient, electrical potential gradient and pressure difference across the membrane. The concentration and the electrical potential gradients give rise to ionic diffusion across the nanofiltration membrane, while pressure difference causes convection of ions across the membrane, (ref. 2).

A model is very important in predicting the membrane performance, understanding the separation mechanism for various substances, selecting the appropriate membrane for a specific application and process design and optimization. In this work, a mathematical modelling of the extended Nernst-Planck equation was used due to its description of the ionic transport mechanisms through nanofiltration membranes and to try to understand nanofiltration membrane separation behaviour, where later it would be compared to an

experimental work. The mathematical model was developed for a negatively charged membrane and one type of electrolyte system, i.e. charged solutes. The charged electrolyte system is in the form of a salt solution containing one anion and one cation species. The existence of a cation and an anion will cause the Donnan effect and consequently affect the separation performance together with the steric effect.

Nernst-Planck equation was solved by using two mathematical methods, which are Euler and Runge-Kutta methods, and the solution was obtained by using FORTRAN program. The two programs were run for different feed concentrations and permeate flux (volume flux based on the membrane area), which were obtained from the experiments. The model was solved for NaCl solution at two different feed concentrations, which were 10 and 100 mol/m^3. For each concentration value, the model was solved for different volume flux values that ranged between 1.0E-7 to 9.0E-6 m^3/m^2/s. These readings were similar to the values used in the experimental work. The change in these parameters values was done to observe their effect on the membrane rejection and if the results obtained from the theory agrees with the results obtained from the experiments. The membrane active layer thickness was assumed to be equal to 20.0E-6 m, which was obtained from the membrane pictures taken by SEM (FEI Quanta 200, Purge, Czech Republic) and EDXS equipment (EDXS, Amertek Inc, Paoli, PA, USA). The pictures for the membrane active layer were taken at different scales.

2 Theory

The extended Nernst-Planck equation covers all of the three important aspects in transport mechanisms through nanofiltration membrane: diffusion, electro-migration and convection. The model development is based on two approaches: the irreversible thermodynamic approach and the hydrodynamic approach, which are governed by both the steric and the charge effects, which in turn govern the ion transport through nanofiltration membrane. The steric effect is caused by the difference between the membrane pore radius and the solute ion radius, while the Donnan effect is actually the result of the charge polarities between the membrane and the solute. These combined effects influence the selectivity of the membrane. The concentration gradient and the electrical potential gradient cause ion diffusion across nanofiltration membranes, whilst the pressure difference causes convection of ions across nanofiltration membrane. Four assumptions were made

- The solution is assumed ideal.
- The membrane charge capacity is uniform.
- All the ions that exist in the membrane are transportable.
- The Donnan equilibrium takes place at the membrane/feed interface, and the membrane/permeate interface.

The extended Nernst-Planck equation is given as

$$j_i = K_{i,c} c_i J_v - D_{i,p} \frac{dc_i}{dx} - \frac{z_i c_i D_{i,p}}{RT} F \frac{d\Psi}{dx} \qquad (1)$$

where j_i is the flux of ion (i) based on the membrane area (mol/m².s), $D_{i,p}$ is the hindered diffusivity (m²/s), c_i is the concentration in the membrane (mol/m³), z_i is the valence of ion (i), $K_{i,c}$ is the hindrance factor for convection inside the membrane, J_v is the volume flux based on the membrane area (m^3/m^2/s), R is the gas constant (J/mol.K), T is the absolute

temperature (K), F is Faraday constant (C/mol) and Ψ is the electrical potential (V). Transport of ions through the membrane is obtained by implying a set of boundary conditions. The ions rejection is calculated by writing the Nernst-Planck equation in the form of concentration and potential gradients. To obtain the concentration gradient, the ion flux is related to its concentration as

$$j_i = C_{i,p} J_v \qquad (2)$$

where $C_{i,p}$ is the concentration of ion (i) in the permeate (mol/m³). Substituting equation (2) into equation (1) and rearranging it gives the concentration gradient as follows

$$\frac{dc_i}{dx} = \frac{J_v}{D_{i,p}}\left(K_{i,c}c_i - C_{i,p}\right) - \frac{z_i c_i}{RT} F \frac{d\Psi}{dx} \qquad (3)$$

To obtain the potential gradient, several conditions were implied. The electro-neutrality conditions are fulfilled in the following order: the feed, the membrane and the permeate, as in equations (4) and (5). The membrane effective charge (X_d) is assumed to be constant and is given as

$$\sum_{i=1}^{n} z_i c_i = -X_d \qquad (4)$$

where X_d is the effective membrane charge density (mol/m³). The electro-neutrality condition in the bulk solution is given as

$$\sum_{i=1}^{n} z_i C_i = 0 \qquad (5)$$

The electro-neutrality condition in the permeate solution is given as

$$\sum_{i=1}^{n} z_i C_{i,p} = 0 \qquad (6)$$

By applying the conditions in equations (4), (5) and (6) for equation (3) and rearranging it, gives the electrical potential gradient as follows

$$\frac{d\Psi}{dx} = \frac{\sum_{i=1}^{n} \frac{z_i J_v}{D_{i,p}}\left(K_{i,c}c_i - C_{i,p}\right)}{\frac{F}{RT}\sum_{i=1}^{n} z_i^2 c_i} \qquad (7)$$

The Donnan equilibrium was assumed to apply at the feed/membrane interface and at the membrane/permeate interface. The Donnan equilibrium is given as

$$\left(\frac{\gamma_i c_i}{\gamma_i^o C_i}\right) = \phi \exp\left(-\frac{z_i F}{RT}\Delta\Psi_D\right) \qquad (8)$$

where γ_i is the activity coefficient of ion (i) in the membrane, γ_i° is the activity of ion (i) in the bulk solution and ϕ is the steric partitioning term. Equation (8) defines the boundary conditions at both sides of the membrane. Assuming an ideal conditions then the steric partitioning was dropped from Donnan equation. Assuming that the solution is dilute then the activity coefficient, to be accounted for inside the membrane by the effective membrane charge density, would be equal to unity. Thus, the Donnan equilibrium becomes as

$$\left(\frac{c_i}{C_i}\right) = \exp\left(-\frac{z_i F}{RT}\Delta\Psi_D\right) \qquad (9)$$

where $\Delta\Psi_D$ is the Donnan potential (V) and C_i is the ion concentration in the solution (mol/m³). Then equations (3) and (7) can be solved over the following conditions

$$at \quad x = 0 \longrightarrow C_i = C_{i,f}$$
$$at \quad x = \Delta x \longrightarrow C_i = C_{i,p}$$

where $C_{i,p}$ is the concentration of ion (i) in the permeate (mol/m³) and $C_{i,f}$ is the concentration of ion (i) in the feed (mol/m³). The rejection (R) of ion (i) is given as

$$R = 1 - \frac{C_{i,p}}{C_{i,f}} \qquad (10)$$

The hindered diffusivity ($D_{i,p}$) and the hindrance factor for convection ($K_{i,c}$) in Nernst-Planck can be obtained from the following equations. The hindered diffusivity is given as follows

$$D_{i,p} = K_{i,d} \cdot D_{i,\infty} \qquad (11)$$

where $D_{i,\infty}$ is the bulk diffusivity (m^2/s) and $K_{i,d}$ is the hindrance factor for diffusion. If the solute velocity inside the membrane pores is taken into consideration then the hindrance factor for convection ($K_{i,c}$) (refs. 1, 4, 5, 10, 16, 17, 18) is given as follows

$$K_{i,c} = (2 - \phi_i) G(\lambda_i, 0) \qquad (12)$$

where G is the hydrodynamic drag coefficient and ϕ is steric partitioning term.

3 Numerical solution

Ion permeation through nanofiltration membrane was described by equations (3), (7) and (9). Equations (3) and (7) were integrated across the membrane active layer thickness and the internal solute concentrations ($c_{i,1}$) is related to the bulk feed concentration ($C_{i,f}$) at the feed/membrane interface and the internal solute concentration ($c_{i,N}$) is related to the permeate concentration ($C_{i,p}$) at the membrane/permeate interface through equation (9).

The feed concentration ($C_{i,f}$) with equation (9) was used to calculate the initial concentration inside the membrane ($c_{i,1}$) and the integration of equations (3) and (7). Then the estimate of the permeate concentration ($C_{i,p}$) was calculated by applying the estimate of ($c_{i,N}$) into equation (9). Then the ion rejection was calculated using equation (10). Two mathematical methods were used to integrate equations (3) and (7): Euler and Runge-Kutta. The permeation of ions through the membrane active layer is illustrated in figure 1.

A value for $d\Psi/dx$ is needed in-order to integrate equation (3), which is a calculation that requires a value of the permeate concentration ($C_{i,p}$). It is therefore reasoning to solve the model in an iterative function using an initial guess for the value of the permeate concentration ($C_{i,p}$). Therefore it was assumed that the initial permeate concentration ($C_{i,p}$) was equal to the feed concentration ($C_{i,f}$) which implies that rejection does not take place. The feed concentration assumed to be equal to the initial feed concentration used in the experiments. The hindered diffusivity ($D_{i,p}$), the hindrance factor for convection inside the membrane ($K_{i,c}$) and the Donnan potential ($\Delta\Psi_D$) were obtained from literature (refs. 4, 16). The solution was assumed to be dilute, as a result the activity coefficient, to be accounted for inside the membrane by the effective membrane charge density, would be equal to unity. The membrane thickness and the membrane pore size were obtained from the membranes used in the experiments. Figure 2 is the programme flowchart.

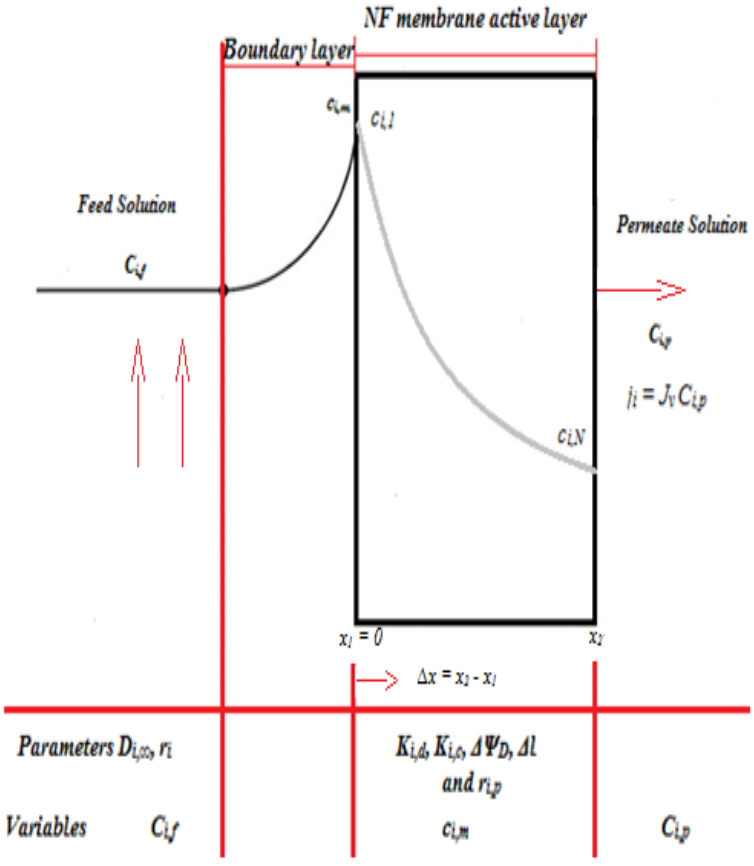

Figure 1. Ion transport through membrane active layer.

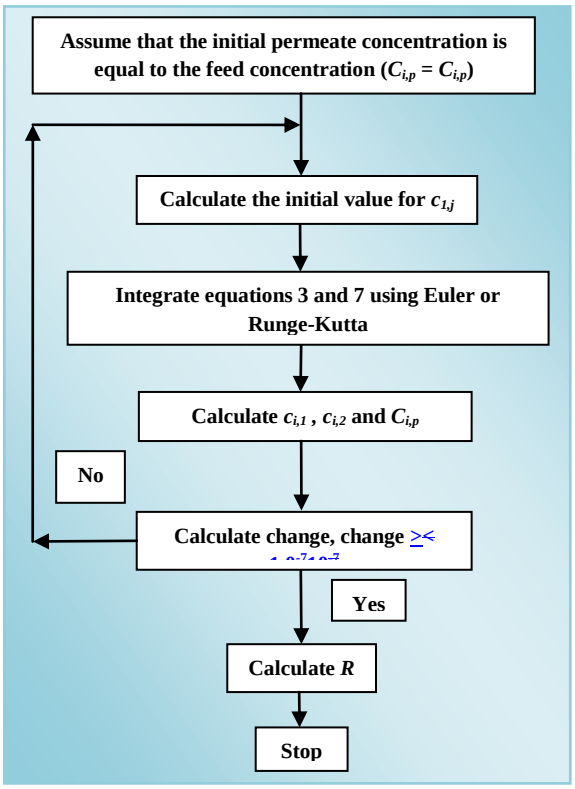

Figure 2. The programme flowchart.

3.1 Euler's numerical method

At the beginning, the initial permeate concentration ($C_{i,p}$) was assumed to be equal to the feed concentration ($C_{i,f}$) to be able to calculate the initial value of the concentration inside the membrane (c_i). Then equation (9) was rearranged and written as

$$c_i = C_{i,f} \exp\left(-\frac{z_i F}{RT}\Delta\Psi_D\right) \qquad (13)$$

where $C_{i,f}$ is the solute concentration in the feed solution. Equation (13) was used to determine the initial solute concentration inside the membrane (c_i) - at the feed/membrane interface - by using the solute feed concentration. Then equation (3) was written according to Euler's method as follows

$$\frac{c_{i,N+1} - c_{i,N}}{\Delta x} = \frac{J_v}{D_{i,p}}\left(K_{i,c}c_{i,N} - C_{i,p}\right) - \frac{z_i c_{i,N}}{RT} F \frac{d\Psi}{dx} \qquad (14)$$

Equation (14) was used to calculate the concentration inside the membrane. Then equation (7) was used to calculate the potential gradient ($d\Psi/dx$), where it was substituted into equation (14) to calculate a new value for the solute concentration inside the membrane. After that, the step-size was assumed to be equal to the membrane active layer thickness over the number of steps, where the number of steps was equal to 200, as in the following equation

$$xstep = \frac{x_2 - x_1}{node} \qquad (15)$$

where *xstep* is the step-size, *node* is the number of steps and *x* is the membrane active layer thickness. The ion concentration inside the membrane active layer changes from $c_{i,1}$ at the feed-solution interface side to $c_{i,200}$ at the permeate-solution interface side. Afterwards, the final concentration inside the membrane was used to calculate the permeate concentration by substituting its value into equation (9.9). The solute concentration in the permeate is given as

$$C_{i,p} = \frac{c_i}{\exp\left(-\frac{z_i F}{RT}\Delta\Psi_D\right)} \qquad (16)$$

where $C_{i,p}$ is the solute concentration in the permeate solution. Then the rejection of ions was calculated using equation (10). The programme would keep running until the difference (change) between the initial and final permeate concentration would be greater than 1.0^{-7}, the change is given as follows

$$change = \frac{c_{i,p} - c_{i+1,p}}{c_{i,p}} \qquad (17)$$

3.2 Runge-Kutta numerical method

At first, the initial permeate concentration was assumed to be equal to the feed concentration in order to calculate the initial value of the concentration inside the membrane. Then the initial concentration inside the membrane was calculated by using equation (13). Afterwards, the potential gradient was calculated by using equation (7). Then the initial concentration inside the membrane and the potential gradient were substituted into equation (3), where it was integrated and gave a new value for the concentration inside the membrane. After that, the step-size was assumed to be equal to the membrane active layer thickness over the number of steps, where the number of steps was equal to 200. The step-size is given as follows

$$h = \frac{x_2 - x_1}{nstep} \qquad (18)$$

where *h* is the step-size, *nstep* is equal to 200 and *x* is the membrane active layer thickness. Where the ion concentration inside the membrane active layer changes from $c_{i,1}$ at the feed-solution side to $c_{i,200}$ at the permeate-solution side. Afterwards, the final concentration inside the membrane ($c_{i,200}$) was used to calculate the permeate concentration. The new value of the solute concentration inside the membrane was used to calculate the solute permeate concentration by substituting it into equation (16). The programme would keep running until the difference (change) between the initial and final permeate concentration would be greater than 0.0000001, as in equation (17).

4 Results

The programs have been run for sodium chloride (NaCl) for two different feed concentration values over a different volume flux based on the membrane area ($m^3/m^2/s$) values. The used concentration values were the same as the values used in the experiments. The initial feed ion concentrations were 10 and 100 mol/m^3. The volume fluxes (based on the membrane area) that were used ranged between 1.0E-7 and 9.0E-6 $m^3/m^2/s$. The membrane thickness was assumed to be equal to 20.0E-6 m, which was the same as that of the used membrane in the experiments.

4.1 Euler method

For both concentration values - 10 and 100 mol/m^3 - it was noticed that the rejection of Na^{+1} and Cl^{-1} ions increased as the volumetric flux based on membrane area (J_v) increased. In addition, the rejection of Cl^{1-} was slightly higher than the rejection of Na^{1+}. See Figures 3, 4, 7 and 8. Such results are supported by the Nernst-Planck equation, where the membrane effective charge (X_d) would have played a role in causing a difference in the rejection between a cation and an anion. The membrane effective charge (X_d) is used as a condition to integrate equation (3) to obtain the electrical potential gradient, also the electrical potential gradient is used to integrate the Nernst-Planck equation to obtain the ions concentration inside the membrane and the permeate solution. It was noticed that the ions rejection increased as the permeate volume flux (based on the membrane area) increased, such observation supports the trans-membrane pressure (TMP) where the theory suggests that the ions rejection would increase as the TMP increases (refs. 2, 7, 8, 9, 11, 14, 17). In addition, the rejection of Na^{+1} and Cl^{-1} ions decreased as the feed concentration increased, (ref. 4). The rejection of Cl^{1-} was higher than the rejection of Na^{1+}. Such rejection behaviour is related to the membrane charge, which is a negative charge. The membrane charge effect would appear in the module in the electrical potential gradient (see equations 4, 5 and 6), which would explain the difference between the rejection of Na^{1+} and Cl^{1-}. Where repulsion between the membrane charge and the Cl^{1-} ions occurs while attraction between the membrane charge and the Na^{1+} ions occurs, which means that Na^{1+} ions would pass more freely through the membrane active layer and the Cl^{1-} ions would be rejected. For the two initial feed concentration values (10 and 100 mol/m^3), it was noticed that the concentration of Na^{1+} and Cl^{1-} ions inside the membrane active layer decreased as the ions moved through the membrane active layer from the feed side to the permeate side. It was noticed that the concentration of Na^{1+} ion inside the membrane active layer was lower than the concentration of Cl^{1-} ion. See Figures 5, 6, 9 and 10. These results are supported by theory where it suggests that the ions concentration decreases as the ions moves through the membrane active layer from the feed/membrane interface to the membrane/permeate interface (refs. 12, 17). Moreover the concentration of the ions inside the membrane active layer decreased as the volumetric flux based on membrane area (J_v) increased, as an example see figure 11, (refs. 12, 17, 18).

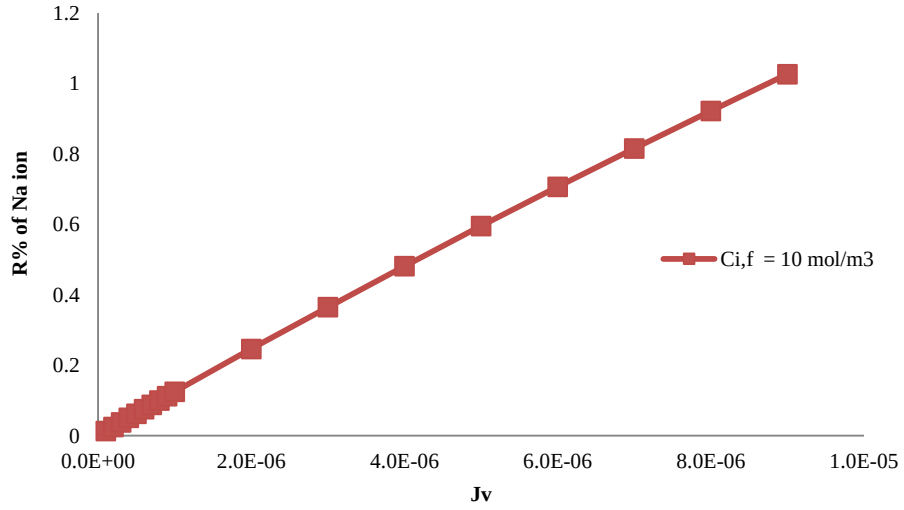

Figure 3. Rejection of Na^{1+} ion versus J_v ($m^3/m^2/s$).

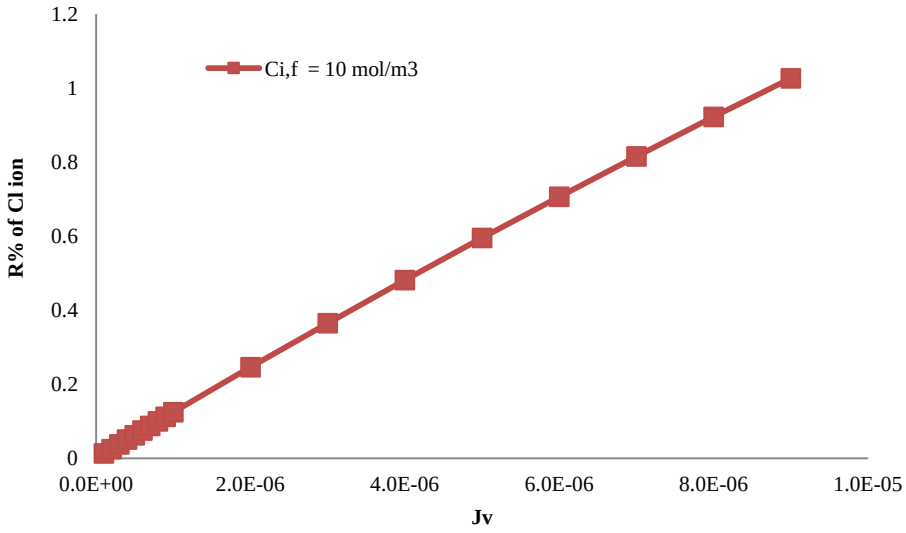

Figure 4. Rejection of Cl^{1-} ion versus J_v ($m^3/m^2/s$).

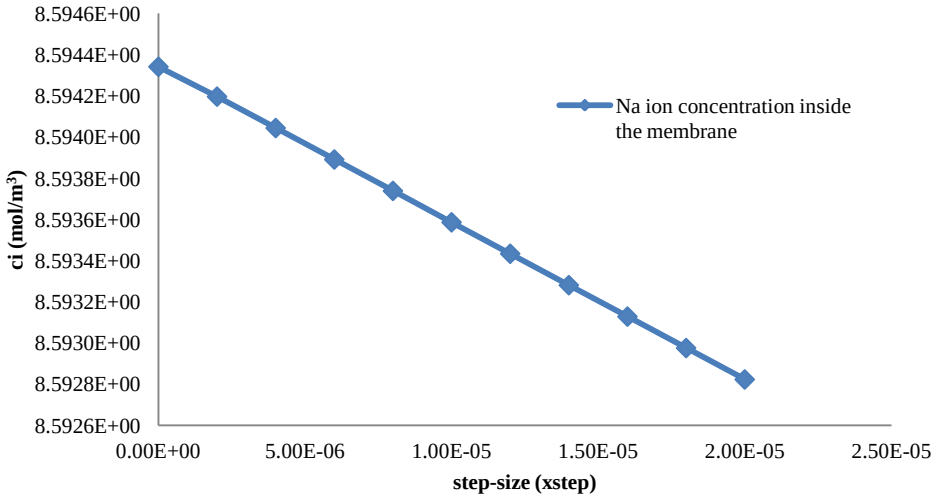

Figure 5. Na^{1+} ion concentration inside the membrane active layer versus the step-size.

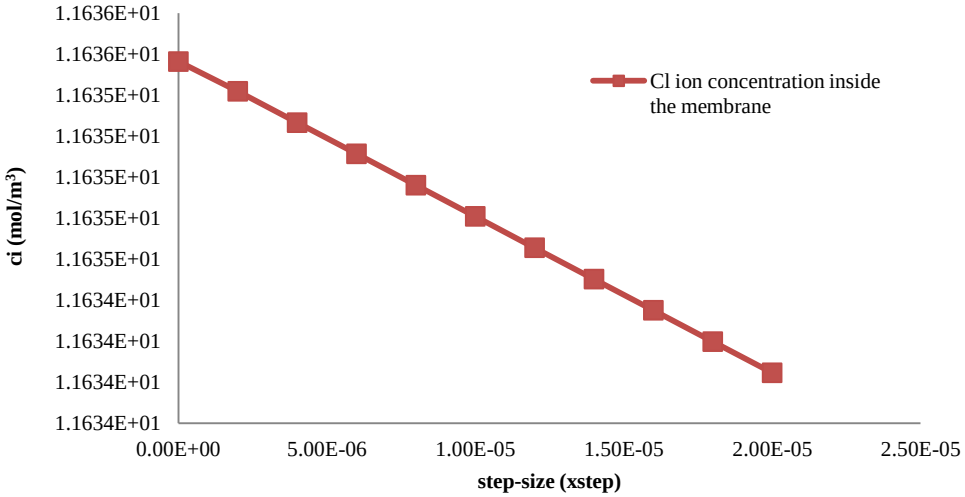

Figure 6. Cl^{1-} ion concentration inside the membrane active layer versus the step-size.

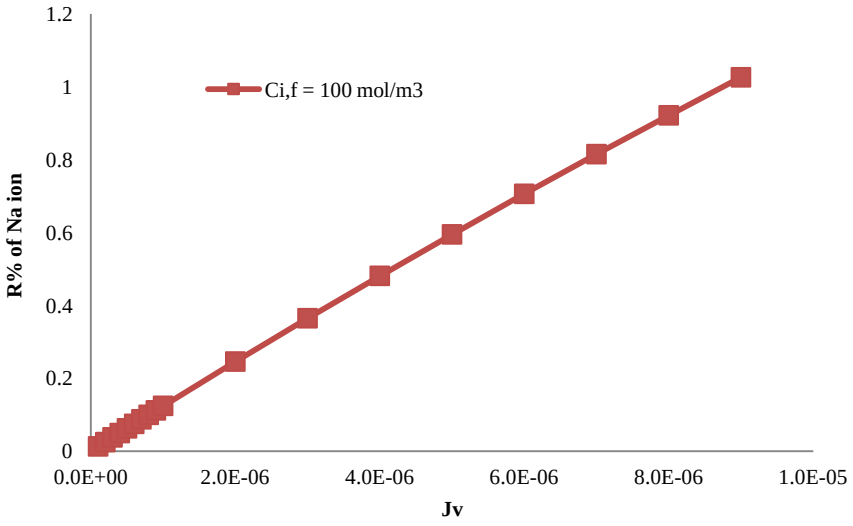

Figure 7. Rejection of Na^{1+} ion versus J_v ($m^3/m^2/s$).

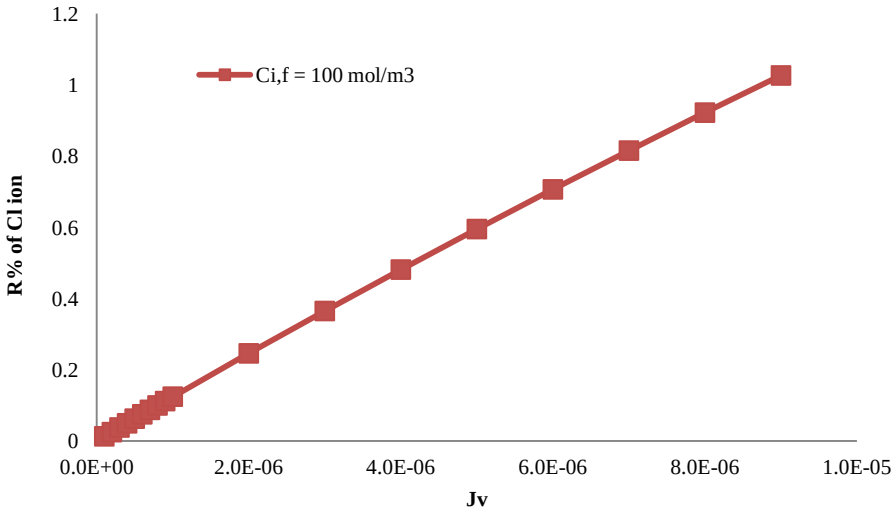

Figure 8. Rejection of Cl^{1-} ion versus J_v ($m^3/m^2/s$).

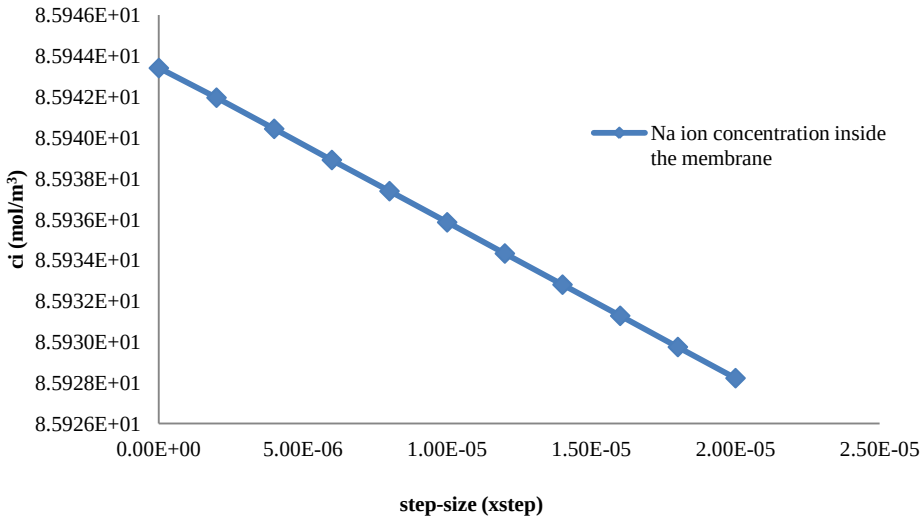

Figure 9. Na^{1+} ion concentration inside the membrane active layer versus the step-size.

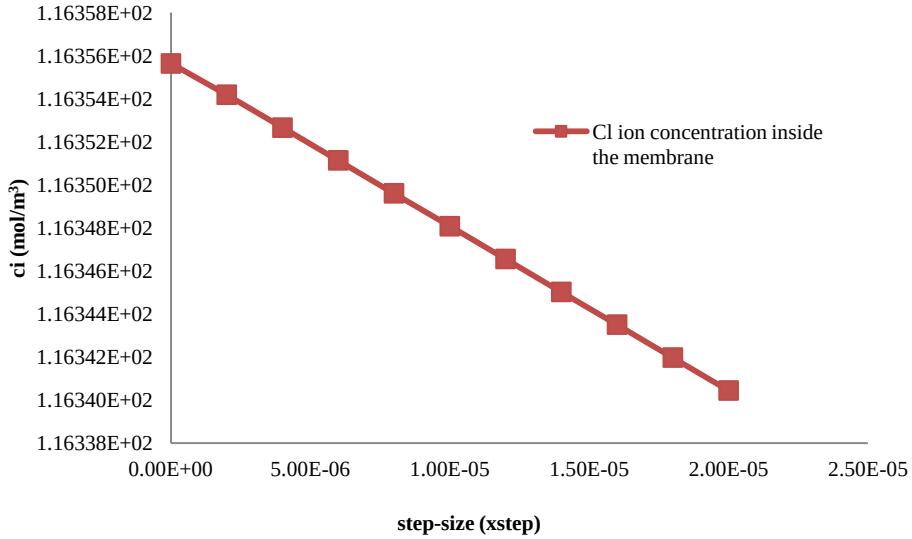

Figure 10. Cl^{1-} ion concentration inside the membrane active layer versus the step-size.

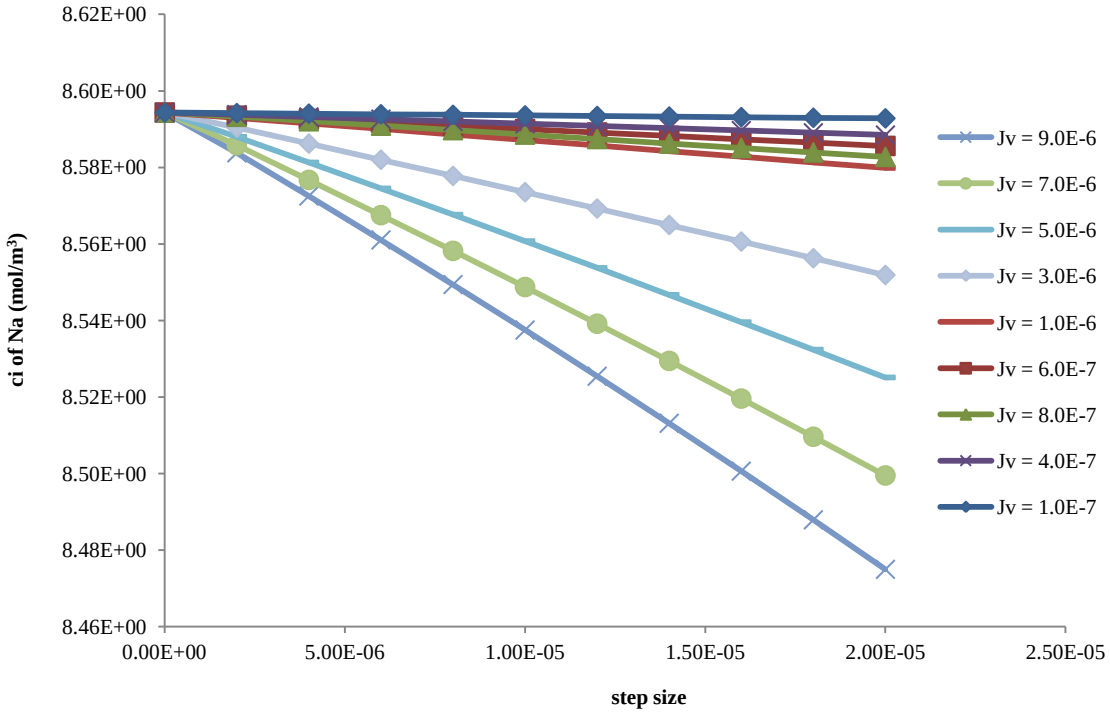

Figure 11. Na^{1+} ion concentration inside the membrane active layer versus the step-size (for different volumetric flux (J_v)).

4.2 Runge-Kutta method

For concentration values it was found that the rejection of Na^{1+} and Cl^{1-} ions increased as the volume flux increased. See Figures 12, 13, 16 and 17. The rejection of Cl^{1-} was slightly higher than the rejection of Na^{1+}. The concentration of Na^{1+} and Cl^{1-} inside the membrane active layer decreased as the ions moved through the membrane active layer from the feed side to the permeate side. See Figures 14, 15, 18 and 19. It was noticed that the concentration of Na^{1+} ion inside the membrane active layer was lower than the concentration of Cl^{1-} ion (refs. 17, 18). The ion's rejection from lower feed ion concentration was slightly higher than the ion's rejection from higher feed ion concentration. This agrees with the theory, because as the ions concentration in the feed solution increases then the ions accumulation on the feed/membrane interface would increase causing the membrane charge effect to decrease and the permeation of ions through the membrane active layer would increase. The rejection of Cl^{1-} was higher than the rejection of Na^{1+}; these results are supported by the Nernst-Planck equation, where the membrane effective charge (X_d) would have played a role in causing a difference in the rejection between a cation and an anion. It was noticed that the ions rejection increased as the permeate volume flux (based on the membrane area) increased, such observation supports the trans-membrane pressure (TMP) where the theory suggests that the ions rejection would increase as the TMP increases. In addition the concentration of the Na^{1+} and Cl^{1-} ions inside the membrane active layer decreased as the volumetric flux based on membrane area (J_v) increased, see figure 20, (refs. 12, 17).

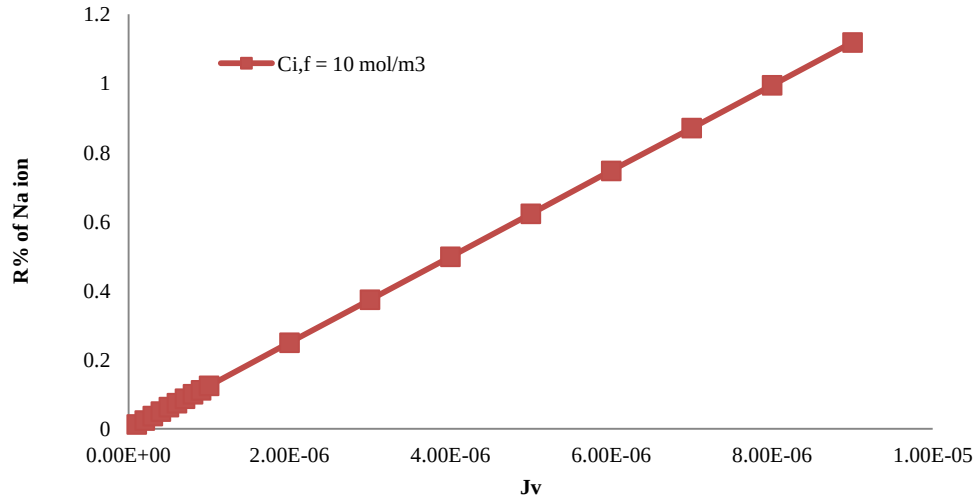

Figure 12. Rejection of Na^{1+} ion versus J_v ($m^3/m^2/s$).

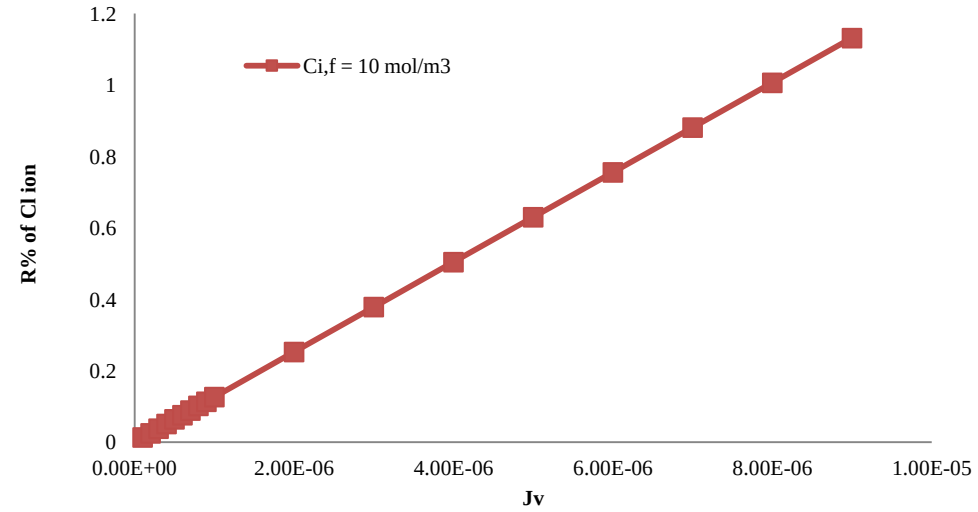

Figure 13. Rejection of Cl^{1-} ion versus J_v ($m^3/m^2/s$).

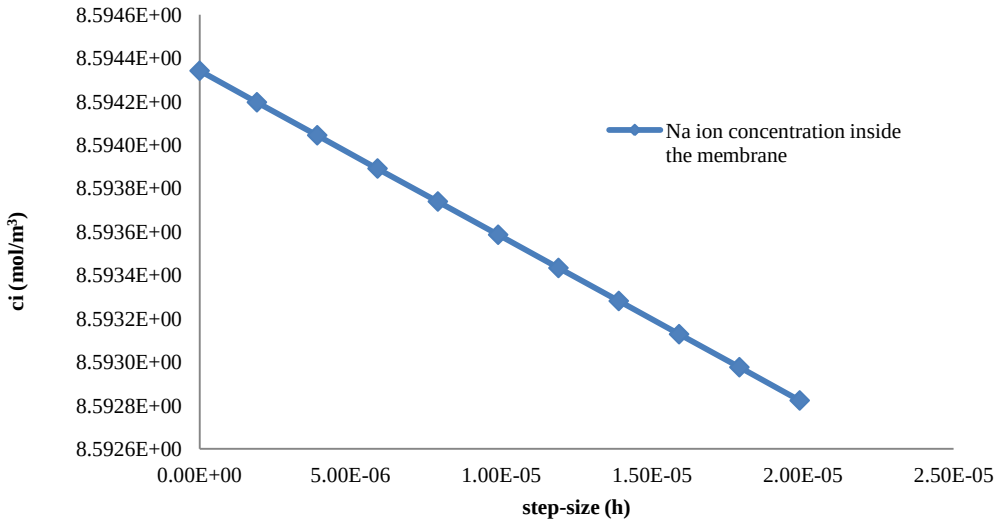

Figure 14. Na^{1+} ion concentration inside the membrane active layer versus the step-size.

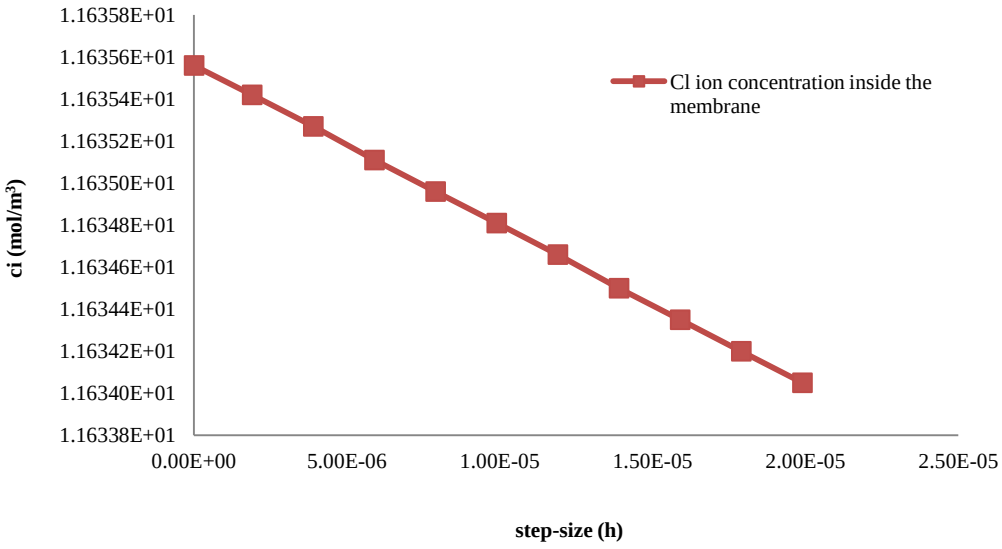

Figure 15. Cl^{1-} ion concentration inside the membrane active layer versus the step-size.

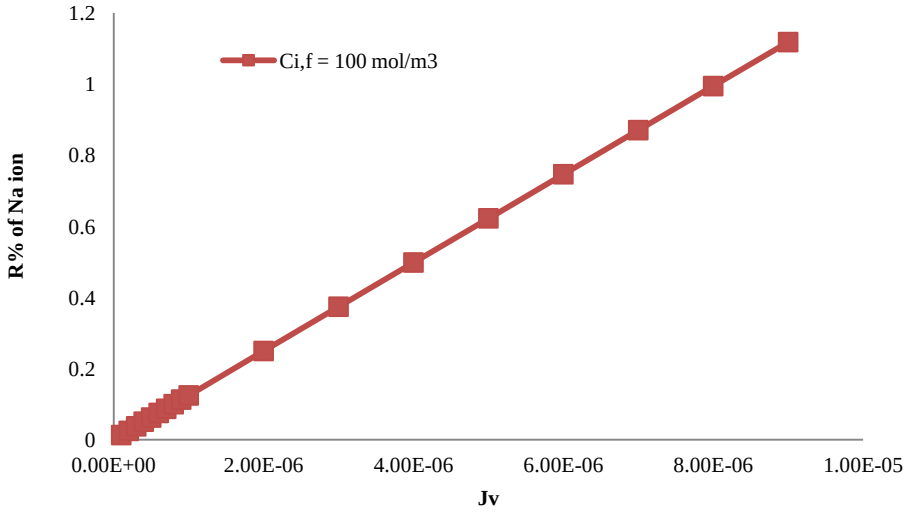

Figure 16. Rejection of Na^{1+} ion versus J_v ($m^3/m^2/s$).

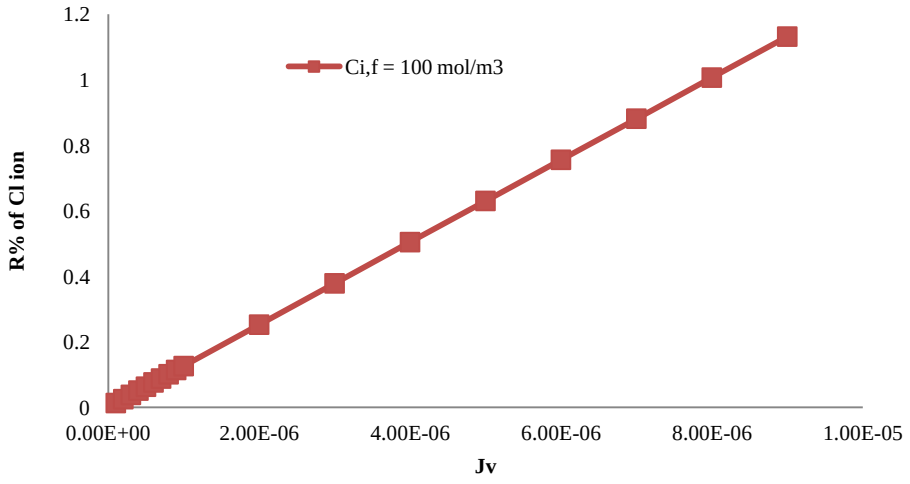

Figure 17. Rejection of Cl^{1-} ion versus J_v ($m^3/m^2/s$).

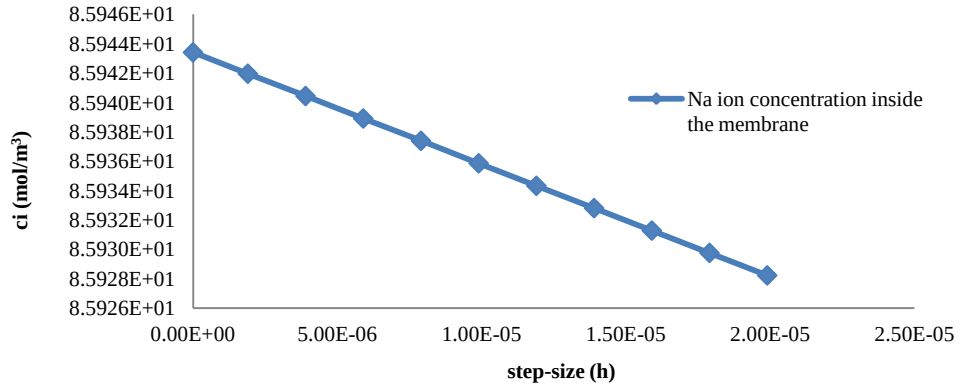

Figure 18. Na^{1+} ion concentration inside the membrane active layer versus the step-size.

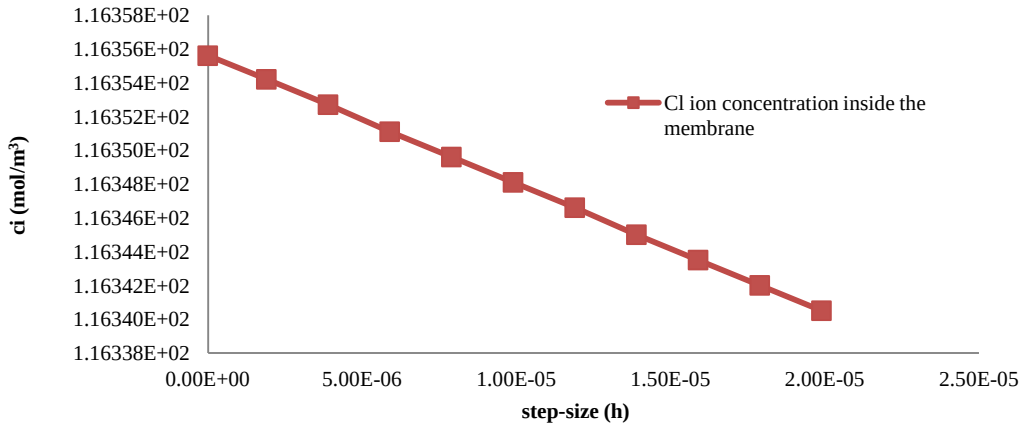

Figure 19. Cl^{1-} ion concentration inside the membrane active layer versus the step-size.

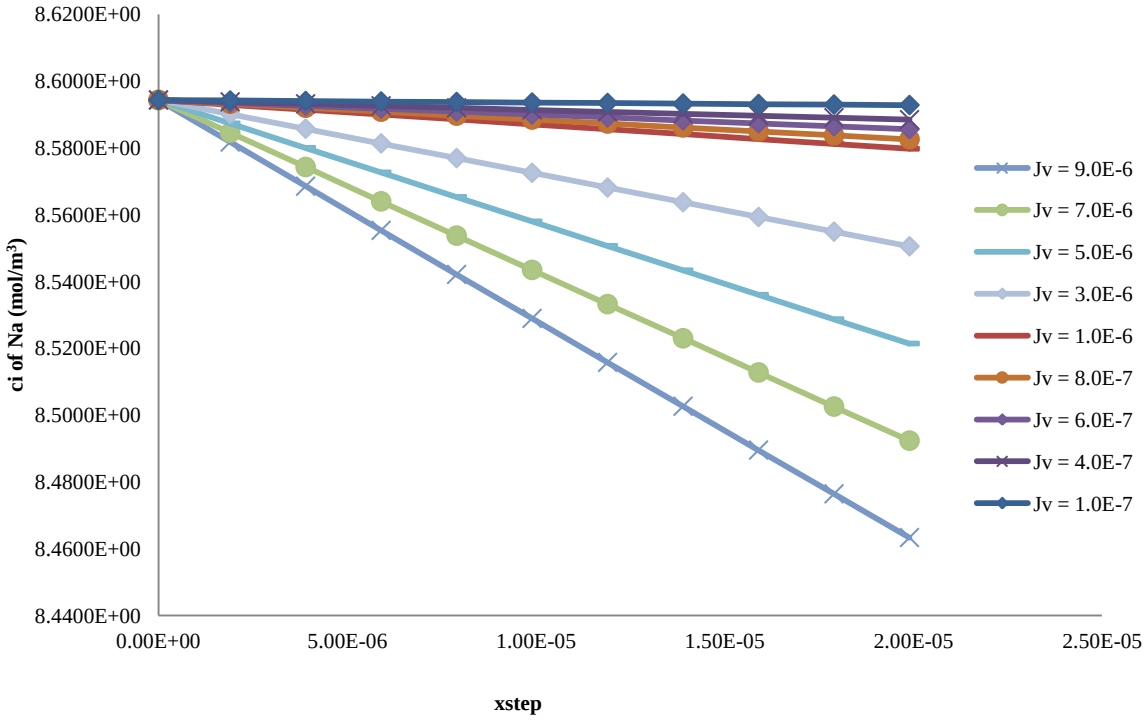

Figure 20. Na^{1+} ion concentration inside the membrane active layer versus the step-size (for different volumetric flux (J_v)).

5 Discussion

The same results were obtained when using the Euler and Runge-Kutta methods. The difference is that the ion's rejection values obtained by using the Runge-Kutta method were slightly higher than the values obtained by the Euler method. Also it was noticed that the rejection of Na^{+1} and Cl^{-1} ions increased as the volumetric flux based on membrane area (J_v) increased. Moreover the concentration of Na^{+1} and Cl^{-1} ions inside the membrane active layer decreased as the volumetric flux based on membrane area (J_v) increased (ref. 12), which supports the increase in the ions rejection as the volumetric flux based (J_v) increases. These results are related to the TMP, where the theory suggests that the ions rejection would increase as the TMP increases (ref. 2). In addition, the rejection of Na^{+1} and Cl^{-1} ions decreased as the feed concentration increased (refs. 4, 17), which was similar to results obtained from the experiments.

The rejection of Cl^{1-} was higher than the rejection of Na^{1+}, which agrees with the results obtained from the experiments. Such rejection behaviour is related to the membrane charge, which is a negative charge. Where the membrane effective charge (X_d) was used as a condition to integrate equation (3) to obtain the electrical potential gradient, as well the electrical potential gradient is used to integrate the Nernst-Planck equation to obtain the ions concentration inside the membrane and the permeate solution (see equations 4, 5 and 6). Repulsion between the membrane charge and the Cl^{1-} ions would occur while attraction between the membrane charge and the Na^{1+} ions would occur, which means that Na^{1+} ions would pass more freely through the membrane active layer and the Cl^{1-} ions would be rejected.

Similar results were obtained by W. Richard Bowen et. al. (refs. 17, 18) over the boundary conditions that were used, where the rejection increased as the volumetric flux based on membrane area (J_v) increased. Moreover when applying the volumetric flux based on membrane area (J_v) that were used in W. Richard Bowen et. al. work, similar results were obtained with the model that was used in this work.

Increasing the membrane thickness increased ions rejection, where the rejection was higher than 40%, which agrees with several works that have been done for nanofiltration membrane. Nevertheless, in this work, the thickness of the membrane active layer was considered as the membrane thickness because it is the main part of the membrane where ions separation occurs. In addition, the pore radius of the support layer is larger than the ions radius thus the ions would pass easily through the support layer; as a result, the support layer thickness can be neglected. However, if large molecules were used with such model then the support layer thickness cannot be neglected because it would have an impact on the rejection of molecules. Runge-Kutta method could solve equation (9.3) when the membrane thickness was assumed to be equal to 1.40E-3 m, which is the actual membrane thickness including the active layer and the support layer. On the other hand, Euler method could not solve equation (3) for a membrane thickness higher than 6.0E-4 m. The accuracy of both models was checked by doubling the step-size, were similar results were obtained.

6 Summary

The calculation method for the Nernst-Planck equation was described. The extended Nernst-Planck equation was solved using Euler and Runge-Kutta mathematical methods. FORTRAN programme was used to solve the model. This model is known for its limitation and for being

more descriptive than predictive, and in-order to overcome these limitations experimental parameters were used. The chosen ions were Na^{1+} and Cl^{1-} ions. The model was solved for two different feed concentrations, which were 10 and 100 mol/m^3. The membrane active layer thickness was assumed to be equal to 20.0E-6 m, which was obtained from the experiments. For each concentration value, the model was solved for different volume flux values that ranged between 1.0E-7 to 9.0E-6 $m^3/m^2/s$. More work need to be done in-order to improve this method such understanding the physics of solutions and the properties of ions because they have great effect on the nanofiltration separation process.

Acknowledgments

The author wishes to gratefully acknowledge and thank the late Dr. Alec E. James — may his soul rest in peace — for his support, supervision, advice, guidance and patience during the research period and writing process. The author also wishes to gratefully acknowledge and thank Dr. Alastair Martin for his excellent advice and help.

References

1) A. I. Cavaco Morão, A. Szymczyk, P. Fievet, A. M. Brites Alves. *Modelling the separation by nanofiltration of a multi-ionic solution relevant to an industrial process*. Journal of Membrane Science 322 (2008) 320–330.
2) A. I. Schäfer, A. G. Fane, T. D. Waite, *Nanofiltration principles and applications*. Oxford : Elsevier, 2005.
3) C. Labbez, P. Fievet, F. Thomas, A. Szymczyk, A. Vidonne, A. Foissy, and P. Pagetti. *Evaluation of the "DSPM" model on a titania membrane: measurements of charged and uncharged solute retention, electrokinetic charge, pore size, and water permeability*. Journal of colloid and interface science 262 (2003) 200–211.
4) J. M. M. Peeters, J. P. Boom, M. H. V. Mulder and H. Strathmann. *Retention measurements of Nanofiltration membranes with electrolyte solutions*. Journal of membrane science 145 (1998) 199–209.
5) Maria Diná Afonso and Maria Norberta de Pinho. *Transport of MgSO4, MgCl2 and Na2SO4 across an amphitricha Nanofiltration membrane*. Journal of membrane science 179 (2000) 137–154.
6) N. Hilal, H. Al-Zoubi, N. A. Darwish, A. W. Mohammad and M. Abu Arabi. *A comprehensive review of Nanofiltration membranes: Treatment, pre-treatment, modelling, and atomic force microscopy*. Desalination 170 (2004) 281–308.
7) Richard Bowen and A. Wahab Mohammad. *Diafiltration by Nanofiltration: prediction and optimisation*. W AIChE journal, volume 44, no. 8 (August 1998) 1799–1812.
8) S. Wadley, C. J. Brouckaert, L. A. D. Baddock, C. A. Buckley. *Modelling of nanofiltration applied to the recovery of salt from waste brine at a sugar decolourisation plant*. Journal of Membrane Science 102 (1995) 163–175.
9) Serena Bandini. *Modelling the mechanism of charge formation in NF membranes: Theory and application*. Journal of membrane science 264 (2005) 75–86.
10) Tim Van Gestel, Carol Vandecasteele, Anita Buekenhoudt, Chris Dotremint, Jan Luyten, Roger Leysen, Bart Van der Bruggen, Guido Maes. *Salt retention in nanofiltration with multilayer ceramic TiO2 membranes.* Journal of membrane science 209 (2002) 379–389.
11) Tsuru, Shin-Ichi Nakao and Shoji Kimura. *Calculation of ion rejection by extended Nernst-Planck equation with charged Reverse osmosis membranes for single and mixed electrolyte solutions*. Journal of chemical engineering of Japan, volume 24, no. 4 (1991) 511–517.

12) Vítor Geraldes, Ana Maria Brites Alves. *Computer program for simulation of mass transport in nanofiltration membranes*. Journal of Membrane Science 321 (2008) 172–182.
13) W. G. J. van der Meer, C. W. Aeijelts Averink, J. C. van Dijk. *Mathematical model of nanofiltration systems*. Desalination 105 (1996) 25–31.
14) W. R. Bowen (Fellow) and A. W. Mohammad. *Characterization and prediction of nanofiltration membrane performance – A general assessment*. Trans IChemE Vol. 76 Part A (November 1998) 885–893.
15) W. Richard Bowen and A. Wahab Mohammad. *A theoretical basis for specifying Nanofiltration membranes - Dye/salt/water streams*. Desalination 117 (1998) 257-264.
16) W. Richard Bowen, A. Wahab Mohammad, Nidal Hilal. *Characterisation of Nanofiltration membranes for predictive purposes use of salts, uncharged solutes and atomic force microscopy*. Journal of membrane science 126 (1997) 91–105.
17) W. Richard Bowen and Hilmi Mukhtar. *Characterisation of prediction of separation performance of Nanofiltration membranes*. Journal of membrane science 112 (1996) 263-274.
18) W. Richard Bowen, Julian S. Welfoot. *Modelling the performance of membrane nanofiltration - critical assessment and model development*. Chemical engineering science 57 (2002) 1121–1137.
19) X. Lefebvre, J. Palmeri, J. Sandeaux, R. Sandeaux, P. David, B. Maleyre, C. Guizard, P. Amblard, J. -F. Diaz, B. Lamaze. *Nanofiltration modeling: a comparative study of the salt filtration performance of a charged ceramic membrane and an organic nanofilter using the computer simulation program NANOFLUX*. Separation and Purification Technology 32 (2003) 117–126.
20) Y. Garba, S. Taha, N. Gondrexon, G. Dorange. *Ion transport modelling through nanofiltration membranes*. Journal of Membrane Science 160 (1999) 187–200.